

Concept Paper

# Solving the Green Open Vehicle Routing Problem Using a Membrane-Inspired Hybrid Algorithm

Yunyun Niu <sup>1</sup>, Zehua Yang <sup>1</sup>, Rong Wen <sup>2</sup>, Jianhua Xiao <sup>3</sup> and Shuai Zhang <sup>4,\*</sup>

<sup>1</sup> School of Information Engineering, China University of Geosciences in Beijing, Beijing 100083, China; yniu@cugb.edu.cn (Y.N.); zhyang1997@163.com (Z.Y.)

<sup>2</sup> Singapore Institute of Manufacturing Technology, Singapore 138634, Singapore; wenr@simtech.a-star.edu.sg

<sup>3</sup> The Research Center of Logistics, Nankai University, Tianjin 300071, China; jhxiao@nankai.edu.cn

<sup>4</sup> DeGroote School of Business, McMaster University, Hamilton, ON L8S 4M4, Canada

\* Correspondence: zhans72@mcmaster.ca

**Abstract:** The green open vehicle routing problem with time windows has been widely studied to plan routes with minimal emissions in third-party logistics. Due to the NP-hardness, the performance of the general heuristics significantly degrades when dealing with large-scale instances. In this paper, we propose a membrane-inspired hybrid algorithm to solve the problem. The proposed algorithm has a three-level structure of cell-like nested membranes, where tabu search, genetic operators, and neighbourhood search are incorporated. In particular, the elementary membranes (level-3) provide extra attractors to the tabu search in their adjacent level-2 membranes. The genetic algorithm in the skin membrane (level-1) is designed to retain the desirable gene segments of tentative solutions, especially using its crossover operator. The tabu search in the level-2 membranes helps the genetic algorithm circumvent the local optimum. Two sets of real-life instances, one of a Chinese logistics company, Jingdong, and the other of Beijing city, are tested to evaluate our method. The experimental results reveal that the proposed algorithm is considerably superior to the baselines for solving the large-scale green open vehicle routing problem with time windows.

**Keywords:** membrane computing; P system; open vehicle routing problem; carbon emission; tabu search



**Citation:** Niu, Y.; Yang, Z.; Wen, R.; Xiao, J.; Zhang, S. Solving the Green Open Vehicle Routing Problem Using a Membrane-Inspired Hybrid Algorithm. *Sustainability* **2022**, *14*, 8661. <https://doi.org/10.3390/su14148661>

Academic Editors: Jianghang Chen, Jie Chu, Jianxin Fang and Yiping Jiang

Received: 12 June 2022

Accepted: 12 July 2022

Published: 15 July 2022

**Publisher's Note:** MDPI stays neutral with regard to jurisdictional claims in published maps and institutional affiliations.



**Copyright:** © 2022 by the authors. Licensee MDPI, Basel, Switzerland. This article is an open access article distributed under the terms and conditions of the Creative Commons Attribution (CC BY) license (<https://creativecommons.org/licenses/by/4.0/>).

## 1. Introduction

The vehicle routing problem (VRP) introduced by Dantzig and Ramser in 1959 [1] is most commonly studied for route planning in logistics. It is defined as the determination of the routes along which a fleet of freight vehicles fulfills the needs of a set of customers (or nodes) at various locations, with the objective of optimising the total cost. Thereafter, a number of VRP variants have been proposed and investigated [2]. Among them, the vehicle routing problem with time windows (VRPTW) has been widely explored, as more practical factors are considered [3]. In this problem, each customer has to be served within their own prescribed time interval, which is named the time window constraint [4].

The open vehicle routing problem with time window (OVRPTW) is a variant of the VRPTW [5]. Compared to the VRPTW, vehicles in the OVRPTW are not required to return to the depot after fulfilling the delivery. This phenomenon is quite popular in many real-world scenarios, where vehicles may not need to return to the depot if they directly finish after serving the customers, especially when a third-party company is delivering. Considering the benefits of higher operation efficiency and the resource utilisation rate, outsourcing freight shipping to third-party logistics companies may have considerable cost savings. Currently, due to the extensive concern about environmental pollution, the logistics industry needs to reduce greenhouse gas emissions [6] to achieve green and sustainable transportation. The OVRPTW is further extended to the green OVRPTW (GOVRPTW), i.e., the objective of the studied problem is to minimise the total greenhouse gas emissions.

The first solution to the open vehicle routing problem (OVRP) was proposed by Bodin et al. [7] in 1983. In that study, a variant of the Clarke and Wright algorithm was designed to develop open routes for airplanes. From then on, various heuristics and metaheuristics have been developed to solve the OVRP. The most widely used are based on a search algorithm, e.g., the tabu search [8], the neighbourhood-based search [9], and the threshold accepting algorithm [10]. Meanwhile, bioinspired and population-based metaheuristics have also been developed, such as the particle swarm optimisation [11], the ant colony optimisation [12], and genetic and evolutionary computing [13].

Recently, Ashtineh and Pishvaei [14] evaluated the economic and environmental impacts of alternative fuels in the VRP through measurement and quantification of the effects for the emitted pollutant. Yu et al. [15] considered a heterogeneous fleet of vehicles to reduce carbon emissions in the green vehicle routing problem with time windows (GVRPTW). Wang and Lu [16] presented a memetic algorithm with competition (MAC) to solve the capacitated green vehicle routing problem. We investigated the fuel consumption in route planning while considering the third-party logistics company, which was formulated based on a comprehensive modal emission model [17]. Specifically, a hybrid tabu search algorithm integrated with several neighbourhood search strategies was leveraged to solve this problem. Although desirable performance was achieved in [17], there is still much room for improvement, especially given that the GOVRPTW is of strong NP-hardness, where the computation becomes prohibitively intractable as the problem scales up.

As a promising branch of the bioinspired intelligent optimisation approach [18], membrane computing has been identified as an effective distributed and parallel model, which is also known as the P system [19]. The theory and applications of the P system and its variants provide a theoretical possibility to solve NP-complete problems in polynomial time [20] and have been widely studied in various fields [21], such as ecosystem and pedestrian behaviour, engineering computing and optimising, and so on. Motivated by those successful applications, we expect that more effective optimisation algorithms could be derived based on the P system for solving GOVRPTW, especially when integrated with evolutionary algorithms. In this paper, we exploit a membrane-inspired hybrid heuristic algorithm to solve the large-scale GOVRPTW to improve the performance over [17], which was based on a hybrid tabu search. The main contributions of this paper are summarised as follows.

- (1) A novel three-level nested membrane structure is designed with respective algorithms. To be specific, the skin membrane acts as the first level, where a genetic algorithm is mainly exploited to search for solutions to the routing problems. Six adjacent inner membranes act as the second level, where different tabu search algorithms are exploited to find tentative solutions. The elementary membrane in each level-2 membrane acts as the third level, where neighbourhood search operations are exploited to facilitate adjusting the search direction of the corresponding level-2 membrane.
- (2) Communication channels between the level-2 membranes and their inner membranes are designed to exchange solutions to favourably find better solutions. Communication channels also exist between the skin membrane and the level-2 membranes, where the crossover operator in the genetic operators is leveraged to retain satisfactory gene segments. In addition, the tabu search with different attractors is adopted to help the genetic algorithm escape from the local optimum. The convergence curve cliffs after each communication justify the effectiveness of the communication channels.
- (3) Experiments are carried out on large-scale real-world problem instances, i.e., a Beijing 100-nodes set and a Jingdong 1000-nodes instance. The results demonstrate that our method significantly outperformed the hybrid tabu search [17], tabu search, and genetic algorithm, respectively. In particular, the computation time observed when comparing the performance on the Jingdong 1000-nodes instances and the Beijing 100-nodes instances further demonstrates the superiority of our algorithm in solving large-scale problems.

## 2. Related Work

### 2.1. Algorithms for the OVRP

Various heuristics and metaheuristics have been developed to solve the OVRP. There is much research on tabu search, neighbourhood-based search, and the threshold accepting algorithm. Brando [8] presented a novel tabu search algorithm for the open vehicle routing problem. Derigs et al. [22] proposed an attribute-based hill climber heuristic, which was a parameter-free variant of the tabu search principle. Fu et al. [23] presented a new tabu search heuristic for finding the routes that minimised two objectives while satisfying three constraints. Russell et al. [24] proposed a tabu search metaheuristic to aid in the coordination and synchronisation of the production and delivery of multiproduct newspapers to bulk delivery locations. Fleszar et al. [9] proposed an effective variable neighbourhood search heuristic. Pisinger et al. [25] presented a unified heuristic with an adaptive large neighborhood search framework to solve five different variants of the VRP. Salari et al. [26] proposed a heuristic improvement procedure based on integer linear programming techniques. Zachariadis et al. [27] presented an innovative local search metaheuristic, which examined wide solution neighbourhoods. Tarantilis et al. proposed an annealing-based method that utilised a backtracking policy [28] and a single-parameter metaheuristic method that exploited a list of threshold values to intelligently guide an advanced local search [10].

Population-based metaheuristics have also been proposed. MirHassani et al. [11] presented a real-value version of particle swarm optimisation for solving the OVRP. Wang et al. [29] proposed a novel real number encoding method of particle swarm optimisation. Zhen et al. [30] proposed a novel particle swarm optimisation in which the vehicle was mapped into the integer part of the real number. Li et al. presented an ant colony system hybridised with local search [31] and an ant colony optimisation-based metaheuristic [12]. Pan et al. [32] presented a clonal selection algorithm. Repoussis et al. [13] proposed a hybrid evolution strategy. Yu et al. [33] applied a novel hybrid algorithm combining the genetic algorithm and the tabu search. The tabu search can help the genetic algorithm circumvent the local optimum. In our previous work, a hybrid tabu search algorithm was proposed to minimise the fuel consumption of the OVRPTW [17]. However, the performance of the algorithms mentioned above always degrades when dealing with a large-scale instance.

### 2.2. Membrane Algorithms

Membrane computing is a branch of natural computing. It is inspired by the structure and the function of living cells, tissues, and organs. It provides a distributed and parallel framework for modelling and high-performance computation. Barbuti et al. [34] proposed minimal probabilistic P systems as modelling notation for ecological systems. Lucie et al. [35] summarised the most important results on P colonies. Niu et al. [36] proposed a simulation model called an intelligence decision P system inspired by the process of cell migration. Sakellariou et al. [37] used a population P system in the agent-based simulation modelling of passengers boarding an underground station.

Nishida T. Y. [38] proposed the first membrane-inspired algorithm and proved its efficiency in solving the travelling salesman problem (TSP). Zhang et al. [39] analysed and optimised radar emitter signals by leveraging membrane algorithms. An optimisation spiking neural P system was presented to approximately solve the general combinatorial optimisation problems [40]. Zhang et al. [41] proposed a population-membrane-system-inspired evolutionary algorithm, in which a population P system and a quantum-inspired evolutionary algorithm were used. Membrane algorithms adopt rich and varied frameworks, which facilitate the cooperation of multiple algorithms. It helps to design a hybrid algorithm and use the respective advantages of different algorithms for large-scale NP-hard problems. In this work, a novel three-level membrane algorithm was designed for the large-scale GOVRPTW instances. It can also be considered an extension of the application field of membrane algorithms.

### 3. Problem Formulation

The problem studied in this paper takes into account practical factors such as vehicle fuel consumption, greenhouse gas emissions, third-party logistics, and time window constraints on the basis of the classical vehicle routing problem, which can be modelled as a green open vehicle routing problem with time window (GOVRPTW). The GOVRPTW could be defined on a complete and directed graph  $\mathcal{G} = (N, A)$ , where  $N$  is the node set and  $A$  is the arc set. In particular,  $N = \{0, \dots, n\}$  includes  $n+1$  entities, with 0 representing the depot and  $N_0 = N \setminus \{0\}$  representing the customer set. Each customer  $i$  has a positive demand  $q_i$ . The arc set  $A = \{(i, j) : i, j \in N, i \neq j, j \neq 0\}$  represents the connection between the nodes. The goods delivery is considered as opposed to the goods pick-up problem. The demand of any customer  $q_i$  is assumed to be less than the vehicle capacity  $Q$ . In this work, it is assumed that the traffic conditions on all roads are uncongested or free-flow such that vehicle speeds can be optimised. The vehicles will finish after completing their service to the customers rather than returning to the depot. The notations used in the problem description are summarised in Notations part. We adopt the comprehensive emissions model developed by Barth et al. [42], Barth et al. [43], and Scora et al. [44] to estimate actual fuel consumption and gas emissions. The objective function of the GOVRPTW is formulated as follows [17].

$$\text{Minimise } \sum_{(i,j) \in A} \lambda f_c k N_e V d_{ij} \sum_{r=1}^R z_{ij}^r / v_{ij}^r \quad (1)$$

$$+ \sum_{(i,j) \in A} \lambda f_c \gamma \alpha_{ij} d_{ij} (w x_{ij} + f_{ij}) \quad (2)$$

$$+ \sum_{(i,j) \in A} \lambda f_c \beta \gamma d_{ij} \sum_{r=1}^R (v_{ij}^r)^2 z_{ij}^r \quad (3)$$

$$+ \sum_{j \in N_0} f_d s_j, \quad (4)$$

where  $\lambda = \zeta / \kappa \psi$ ,  $\gamma^h = 1/1000 n_{tf} \eta$  and  $\alpha = \tau + g \sin \theta + g C_r \cos \theta$  are constants;  $\beta = 0.5 C_d \rho A$  is a vehicle-specific constant; the values of the parameter used in the formulation are given in Table 1, and the reader can refer to Koc et al. [45] for more details. The length of arc  $(i, j) \in A$  is denoted by  $d_{ij}$ ; the total weight of a vehicle on arc  $(i, j)$  is calculated as  $w + f_{ij}$ , with  $w$  being the weight of a vehicle and  $f_{ij}$  being the amount of freight flow on arc  $(i, j) \in A$ ; the binary variable  $x_{ij}$  equals 1 if a vehicle travels along the arc  $(i, j) \in A$ , and it is 0 otherwise; and the binary variable  $z_{ij}^r$  equals 1 if a vehicle  $r$  ( $r = 1, 2, \dots$ ) travels along the arc  $(i, j) \in A$  at speed  $v_{ij}^r$ , and it is 0 otherwise. The objective is to minimise the total cost of three components: the fuel consumption, the CO<sub>2</sub> emissions, and the total wage of drivers. The cost induced by the fuel consumption and CO<sub>2</sub> emissions is represented by the first three terms in the objective. Specifically, term (1) describes the engine module cost, term (2) computes the weight module cost, and term (3) reflects the speed module cost. The cost of the driver wage is represented by the fourth term in the objective. The constraints of the GOVRPTW are shown as follows.

$$\sum_{j \in N_0} x_{0j} \leq |N_0|, \quad (5)$$

$$\sum_{i \in N} x_{ij} = 1, \quad \forall j \in N_0 \quad (6)$$

$$\sum_{j \in N} x_{ij} \leq 1, \quad \forall i \in N_0 \quad (7)$$

$$\sum_{i=1}^n x_{i0} = 0, \quad (8)$$

$$\sum_{j \in N} f_{ij} - \sum_{j \in N} f_{ji} = q_i, \forall i \in N_0 \quad (9)$$

$$q_j x_{ij} \leq f_{ij} \leq (Q - q_i) x_{ij}, \forall (i, j) \in A \quad (10)$$

$$y_i - y_j + t_i + \sum_{r=1}^R d_{ij} z_{ij}^r / v_{ij}^r \leq M_{ij} (1 - x_{ij}), \forall i \in N, j \in N_0, i \neq j \quad (11)$$

$$a_i \leq y_i \leq b_i, \forall i \in N_0 \quad (12)$$

$$\sum_{r=1}^R z_{ij}^r = x_{ij}, \forall (i, j) \in A \quad (13)$$

$$x_{ij} \in \{0, 1\}, \forall (i, j) \in A \quad (14)$$

$$z_{ij}^r \in \{0, 1\}, \forall (i, j) \in A, r = 1, \dots, R \quad (15)$$

$$f_{ij} \geq 0, \forall (i, j) \in A \quad (16)$$

$$y_i \geq 0, \forall i \in N_0 \quad (17)$$

$$s_i \geq 0, \forall i \in N_0 \quad (18)$$

where  $t_i$  is the time consumed for serving customer  $i \in N_0$ ;  $[a_i, b_i]$  is the time window of customer  $i \in N_0$ , within which the customer must be visited;  $y_j$  is the actual starting time for serving node  $j \in N_0$ ; if a vehicle arrives at a customer before its  $a_i$ , it has to wait because it can only start service at or after  $a_i$ ;  $s_j$  is the total time cost of the route in which the last visited customer is  $j \in N_0$ . Moreover, constraint (5) defines the maximum number of vehicles; constraints (6)–(8) ensure that every customer is served only once, and the vehicles finish after delivery rather than returning to where they started; constraints (9) and (10) together define the freight flows; the time window is described in constraints (11) and (12), in which  $M_{ij} = \max\{0, b_i + t_i + d_{ij}/v_{ij}^r - a_j\}$ ; constraint (13) imposes that each arc has only one speed level; and constraints (14)–(18) define the range of the variables.

**Table 1.** Parameter values of a light-duty vehicle.

Notation	Description	Typical Value
$\eta$	Diesel engine efficiency	0.45
$C_r$	Rolling resistance coefficient	0.01
$\rho$	Density of air (kg/m <sup>3</sup> )	1.2041
$\psi$	Conversion factor (g/s to litre/s)	737
$\kappa$	Heating value of the typical diesel fuel (kilojoule/g)	44
$g$	Constant of gravitation (m/s <sup>2</sup> )	9.81
$n_{if}$	Vehicle drive train efficiency	0.45
$\zeta$	Fuel-to-air mass ratio	1
$\tau$	Acceleration (m/s <sup>2</sup> )	0
$\theta$	Angle of the road	0
$v^u$	Highest speed (m/s)	27.8 (or 100 km/h)
$v^l$	Lowest speed (m/s)	5.5 (or 20 km/h)
$f_c$	Cost of fuel and CO <sub>2</sub> emissions (GBP/litre)	1.4
$f_d$	Cost of driver wage (GBP/s)	0.0022

Table 1. Cont.

Notation	Description	Typical Value
$Q$	Vehicle capacity (kg)	4000
$w$	Vehicle curb weight (kg)	3500
$f$	Vehicle fixed cost (GBP/day)	0
$V$	Engine displacement (litre)	4.5
$k$	Engine friction factor (kilojoule/rev/litre)	0.25
$N_e$	Engine speed (rev/s)	38.34
$A$	Area of frontal surface (m <sup>2</sup> )	7.0
$C_d$	Aerodynamics drag coefficient	0.6

#### 4. The Proposed Method

In this section, a membrane-inspired hybrid heuristic algorithm is proposed to deal with the GOVRPTW. As depicted in Figure 1, the MIHA has three levels of cell-like nested membranes. To be specific, the skin membrane constitutes the first level. The second level consists of six adjacent inner membranes (labelled as 1, . . . , 6). The elementary membrane in each level-2 membrane constitutes the third level. The membranes of level-2 can provide the tentative solutions to the skin membrane through unidirectional channels, while the communication channels between the level-2 membranes and the corresponding level-3 membranes are bidirectional. In the membranes of level-3, the neighbourhood search operations are leveraged to help adjust the search direction of the corresponding level-2 membranes. On the one hand, the GA operators in the skin membrane, especially the crossover operator, are exploited to retain the desired gene segments. On the other hand, the tabu search algorithms with different attractors in the level-2 membranes are leveraged to help the GA algorithm escape from the local optimum.

The general framework of the MIHA is introduced in Algorithm 1. In the initialisation stage, the preliminary solutions are generated by using six different operators. Afterwards, a speed improvement strategy is exploited to determine the optimal speed on each route in the solution. In this case, the initial population would be generated in the skin membrane. The searching processes in the level-2 membranes are guided by the tabu search algorithm, while the evolution in the skin membrane proceeds according to the genetic operators. After every  $I_{MCA}$  steps, the archive solutions of each level-2 membrane would be transferred to the skin membrane to help update the current population. When the termination condition is met, the final output is defined as the best solution found from all different membranes.

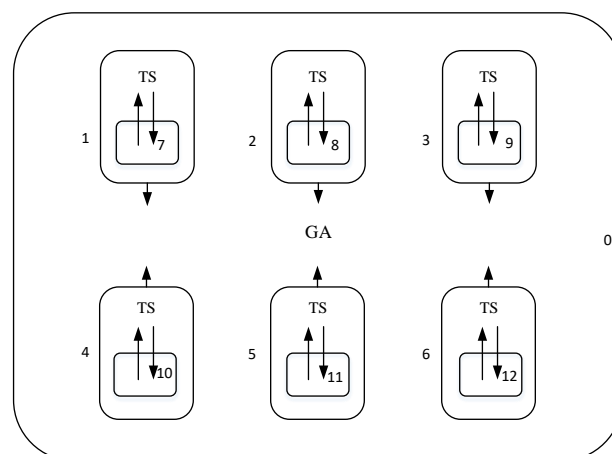


Figure 1. The proposed membrane structure.

**Algorithm 1** Pseudo-code of MIHA**Require:** maximum number of iterations  $I_{max}$ , iteration number before MCA  $I_{MCA}$ **Ensure:**  $x_{best}$ .

```

1: for  $m = 1$  to 6 do
2:   Generate initial solution  $x_{initial}^m$  by using operator  $m$ 
3:   Send  $x_{initial}^m$  to level-2 membrane  $m$ 
4:   Set  $x_{current}^m = x_{initial}^m$ 
5: for  $i = 1$  to  $I_{max}$  do
6:   for  $m = 1$  to 6 do
7:      $\{x_{neighbors}\} = \text{level2\_search}(x_{current}^m)$ 
8:      $\text{update}(\text{archive}^m, \{x_{neighbors}\})$ 
9:     Send  $\{x_{neighbors}\}$  to the adjacent  $\text{level3\_membrane}$ 
10:     $\{x_{neighbors}\} = \text{level3\_search}(\{x_{neighbors}\})$ 
11:     $\text{update}(\text{archive}^m, \{x_{neighbors}\})$ 
12:    if  $\text{archive}^m \setminus \text{tabu\_list}^m \neq \emptyset$  then
13:      Set  $x_{current}^m = \text{the\_best\_of}(\text{archive}^m \setminus \text{tabu\_list}^m)$ 
14:       $\text{update}(\text{tabu\_list}^m, x_{current}^m)$ 
15:   if  $i \bmod I_{MCA} == 0$  then
16:     MCA( $\text{skin\_membrane}$ ,  $\text{level2\_membrane}^{1-6}$ )
17: Output the best solution  $x_{best}$ 

```

The encoding approach of the solution has a significant impact on the quality of the final result as well as the computational efficiency. In our method, a complete solution consists of a number of routes, and the variable-length chromosomes [46] are adopted to encode the routes, where a chromosome comprising the integer nodes represents a route. Specifically, each vehicle departs from the first node and ends at the last node it serves; the travel speed  $v_{ij}^r$  between every two adjacent points  $i$  and  $j$  on the same path is to be decided; the service start time  $y_i$  of each point  $i$  can be calculated; a solution is feasible only when it does not violate any constraints.

#### 4.1. Initialisation

During initialisation, six unique operators were adopted to create different initial solutions as shown in Figure 2. Then, the population of the skin membrane and the archive solutions of the level-2 membranes were formed. Specifically, the six operators were executed based on the following heuristics (or rules). Moreover, the pseudo-code is given in Algorithm 2.

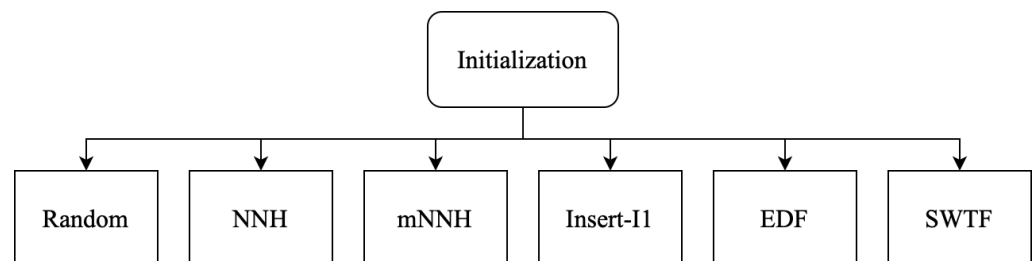


**Figure 2.** Six operators for initialising solutions.

**Algorithm 2** Pseudo-code of initialisation**Require:** Operators: Random, NNH, mNNH,  $I_1$ , EDF, SWTF**Ensure:** Implement the initialisation of MIHA

- 1: operators = {Random, NNH, mNNH,  $I_1$ , EDF, SWTF}
- 2: **for**  $m = 1$  to 6 **do**
- 3:    $x_{initial}^m = \text{create\_initial\_solution}(\text{operator}[m])$
- 4:   Send  $x_{initial}^m$  to *level2\\_membrane* <sup>$m$</sup>
- 5:    $\{x_{neighbors}^m\} = \text{level2\_search}(x_{initial}^m)$
- 6:   Send  $\{x_{neighbors}^m\}$  to *skin\\_membrane*

- (1) Random heuristic: It randomly chooses routes that satisfy constraints (5)–(17).
- (2) Nearest neighbourhood heuristic (NNH): It generates a set of routes according to the distance from the current node. The nearest customer to the depot is chosen as the start node  $x_0$  of the first route. Then it chooses an unassigned customer  $x_1$ , who is nearest to  $x_0$ . It repeats the same procedure until no feasible candidate nodes for the current route can be found. This also means that the current route is completed. Then, it allocates a new vehicle for the next route and constructs the route in a similar way until all customer nodes are assigned.
- (3) Modified nearest neighbourhood heuristic (mNNH): It generates a set of routes according to both the demand of the next customer and the distance from the current node. During the shipping process, a vehicle can offload  $q_i$  payload after servicing customer  $i$ . The unit distance payload of customer  $j$  on arc  $(i, j)$  is defined as  $\overline{\Delta f_{ij}} = q_j / d_{ij}$ . The mNNH creates a number of routes sequentially by considering the  $\overline{\Delta f_{ij}}$  as an objective. First, it chooses the customer  $c$  that satisfies  $c = \text{argmax}_{c \in N_{ucs}} \{|\overline{\Delta f_{0c}}|\}$ , where  $N_{ucs}$  represents the unassigned customer set, which includes the initial current node of the first route. Next, the feasible customer  $nc$  that satisfies  $nc = \text{argmax}_{nc \in N_{ucs}} \{|\overline{\Delta f_{c,nc}}|\}$  is selected as the next node  $c$  and added to the current route. Then, it repeats choosing the next node and appending it to the current route. If no more feasible nodes can be added, the current route is completed, and another route will be constructed in a similar way until all customers have been assigned.
- (4) Insert  $I_1$  heuristic: As first proposed by Solomon [47], the customer  $u^*$  is chosen based on the Equations (19) and (20) and then inserted to the route according to the insert  $I_1$  heuristics. Moreover, the feasible and desired position of the selected  $u^*$  in the route is decided by Equations (21) and (22) as follows, where  $y_{ju}$  is the new time for service to begin at customer  $j$ , given that  $u$  is on the route. The main idea is to use several criteria to insert a new customer into the current partial route at every iteration.

$$c_2(i^*, u^*, j^*) = \text{maximum}[c_2(i, u, j)], \quad (19)$$

$$c_2(i, u, j) = \lambda d_{0u} - c_1(i, u, j), \quad \lambda \geq 0 \quad (20)$$

$$c_1(i^*, u, j^*) = \text{min}[c_1(i, u, j)], \quad (21)$$

$$c_1(i, u, j) = \alpha_1(d_{iu} + d_{uj} - \mu d_{ij}) + \alpha_2(y_{ju} - y_j), \quad \mu, \alpha_1, \alpha_2 \geq 0, \quad \alpha_1 + \alpha_2 = 1. \quad (22)$$

- (5) Earliest deadline first heuristic: It selects the customer with the earliest (or tightest) deadline for service at each step.
- (6) Shortest waiting time first heuristic: It selects the customer with the shortest waiting time.

**4.2. GA in Skin Membrane**

After the initialisation, the population in the skin membrane evolved according to the rationale of GA. To select parent chromosomes for the crossover operator, the binary tournament was implemented, while the chromosomes for the mutation operators were randomly selected.

This process was repeated several times to obtain sufficient parent chromosomes. Route-exchange crossover [46] was used to retain the better gene segment. The routes in one solution chromosome were reproduced and shared with others. In order to satisfy the constraints, the duplicated nodes in a chromosome were removed if a new route was inserted into it. The single point mutation was adopted as the mutation operator in the skin membrane.

#### 4.2.1. Crossover Operator

The performance of the genetic algorithm is highly affected by the crossover and mutation operators. Using these operators, the search space can be more effectively explored and better solutions can be exploited. In the literature of the genetic algorithm, many crossover and mutation operators have been developed for different optimisation problems. In our method, the route-exchange crossover proposed by [46] was adopted to retain the desirable gene segment. Different from the classical one-point crossover, which may produce infeasible route sequences, the route-exchange crossover operator allows the favourable sequences of routes or the genes in a chromosome to be shared with other chromosomes in the evolving population. Firstly, we selected parents to perform the crossover operation by binary tournament. Secondly, the route-exchange crossover was performed on the selected parents, in which the best routes of the selected chromosomes were exchanged. To ensure the feasibility of chromosomes after the crossover, duplicated customers were deleted from the original routes, while the newly inserted route was left unchanged.

#### 4.2.2. Mutation Operator

We adopted three mutation operators, i.e., random, split-longest, and merge-shortest operators [46] to extend the search space. The corresponding operators are listed as follows.

- (1) Random: This operation randomly removes a customer node from a given route and inserts it into another feasible position of the origin route.
- (2) Split-longest: This operation searches for the route with the highest total cost and breaks the route into two parts at a random point.
- (3) Merge-shortest: This operation searches for the two routes of the chromosome with the smallest total cost and appends one to the other.

#### 4.3. Tabu Search in Level-2 Membranes

After the initialisation, the tabu search was started in each level-2 membrane as described in Figure 3 and Algorithm 3. First, the current solution was used to create the neighbour solutions. If any neighbour solution was better than the solutions in the archive, it replaced the most inferior one. Next, the level-3 membrane performed the neighbourhood search and the corresponding result helped the archive to find better solutions. Then, the best one was selected as the next solution from the archive rather than from the tabu list. Finally, the current solution was added into the tabu list.

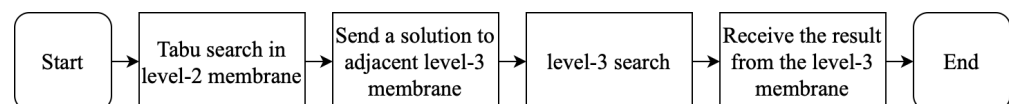


Figure 3. Level-2 membrane search.

Pertaining to the neighborhood search, three operators were exploited.

- (1) Random operator: It randomly exchanges the position of two nodes of a given solution, provided that no constraint is violated.
- (2) High-cost-node operator: It removes a high-cost customer node defined as  $u^* = \operatorname{argmax}_{u \in N} \{d_{iu} + d_{uj}\}$ , where  $i$  is the preceding customer and  $j$  is the succeeding customer, and inserts the node into another position.
- (3) Long-wait-time operator: It relocates the customer with a long wait time node defined as  $u^* = \operatorname{argmax}_{u \in N} \{a_u - e_u\}$ , where  $e_u$  is the arrival time of customer  $u$ .

**Algorithm 3** Level-2 Membrane Search Algorithm

- 1:  $\{x_{neighbors}\} = \text{search\_neighbors}(x_{current})$
- 2:  $\text{update\_its\_archive}(\{x_{neighbors}\})$
- 3: Send  $\{x_{neighbors}\}$  to the adjacent *level3\_membrane* for level-3 search
- 4: **if**  $\text{archive} \setminus \text{tabu\_list} \neq \emptyset$  **then**
- 5:     Set  $x_{current} = \text{the\_best\_of}(\text{archive} \setminus \text{tabu\_list})$
- 6:      $\text{update\_its\_tabu\_list}(x_{current})$

**4.4. Neighbourhood Search in Level-3 Membranes**

In the level-3 membrane, the neighbourhood search was performed with a specific probability, which is denoted as  $p_{level3}$ , to find the superior solutions and improve the diversity of the archive solutions, as illustrated in Figure 4 and Algorithm 4. First, it randomly selected a solution from the archive of the adjacent level-2 membrane. Next, it used this solution as an input to perform the neighbourhood search. Finally, it sent the output of the neighbourhood search back to its adjacent level-2 membrane. If the output solutions were better than the ones in the archive of the level-2 membrane, they replaced the inferior ones. This search procedure is expected to find superior solutions as well as improve the diversity of archive solutions.

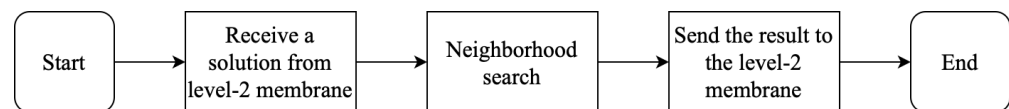


**Figure 4.** Level-3 membrane search.

**Algorithm 4** Level-3 Membrane Search Algorithm

- 1: Randomly select a solution from the archive of adjacent *level2\_membrane*, as  $x_{random}$
- 2: Send  $x_{random}$  to current *level3\_membrane*
- 3:  $\{x_{neighbors}\} = \text{search\_neighbors}(x_{random}, p_{level3})$
- 4: Send  $\{x_{neighbors}\}$  back to the *level2\_membrane*
- 5:  $\text{update}(\text{archive}_{level2\_membrane}, \{x_{neighbors}\})$

**4.5. Communications between the Level-2 Membrane and Skin Membrane**

After a specific number of iterations each time, archive solutions in each level-2 membrane were transported to the skin membrane, and the current population was updated. We denote this number of iterations as  $I_{MCA}$  and this communication as Membrane Communication Algorithm (MCA) (described in Figure 5 and Algorithm 5). First, the archive solutions of each level-2 membrane were merged with current individuals in the skin membrane. Next, the best  $P$  solutions were selected and combined to form a new population. Specifically, the GA operators implemented in the skin membrane, especially the crossover operators, were used to retain the desirable gene segments of solutions found by the tabu search in the level-2 membrane. Various solutions obtained by the tabu search algorithms with different attractors facilitated the GA escaping from the local optimal solutions.

**Algorithm 5** Membrane Communication Algorithm

- 1: **for**  $m = 1$  to 6 **do**
- 2:     Send archive solutions of  $\text{level2\_membrane}[m]$  to *skin\_membrane*
- 3:     Select the best  $P$  solutions in *skin\_membrane*
- 4:     Rebuild the population of *skin\_membrane* with those solutions

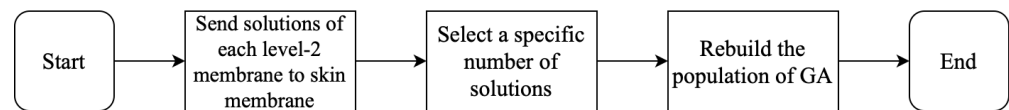


Figure 5. Membrane communication.

#### 4.6. Speed Optimisation

The speed of the vehicle in each arc has a significant impact on the fuel consumption and the total cost. The process of determining the optimal speed of each route in a solution is important to minimise the fuel consumption costs and driver wages. After obtaining a solution that comprised a number of routes, we implemented the speed and departure-time optimisation (SD-TOA) proposed by Karmer et al. [48] to compute the optimal speed for each route. As shown in Algorithm 6, the SD-TOA was executed based on a divide-and-conquer strategy. To be specific, the whole route was divided into several subroutes by first ignoring the time window constraints, and then the sub-routes were re-optimised recursively. If a resulting subroute satisfied all time window constraints, then it was returned. Otherwise, the customer with the maximum time-window violation was identified and its arrival time was set to the closest feasible value. Fixing this time window failure created two subroutes, which were re-optimised recursively.

---

#### Algorithm 6 Speed and Departure-time Optimisation Algorithm (SDTOA)

---

```

1: Procedure SDTOA( $s, e$ )
2:  $p \leftarrow violation \leftarrow maxViolation \leftarrow 0$ 
3:  $D \leftarrow \sum_{i=s}^{e-1} d_{i,i+1}$ 
4:  $T \leftarrow \sum_{i=s}^{e-1} \tau_i$ 
5: if  $s = 1$  and  $e = n_\sigma$  then
6:    $t_1 = a_1$ 
7: if  $e = n_\sigma$  then
8:    $t_e = \min\{\max\{a_e, t_s + D/v_{FD}^* + T\}, b_e\}$ 
9: if  $s = 1$  then
10:   $t_s = \min\{\max\{a_s, t_e - D/v_{FD}^* - T\}, b_s\}$ 
11:  $v_{REF} \leftarrow D/(t_e - t_s - T)$ 
12: for  $i = s + 1 \dots e$  do
13:   $t_i = t_{i-1} + \tau_{i-1} + d_{i-1,i}/v_{REF}$ 
14:   $violation = \max\{0, t_i - b_i, a_i - t_i\}$ 
15:  if  $violation > maxViolation$  then
16:     $maxViolation = violation$ 
17:     $p = i$ 
18:  if  $maxViolation > 0$  then
19:     $t_p = \min\{\max\{a_p, t_p\}, b_p\}$ 
20:    SDTOA( $s, p$ )
21:    SDTOA( $p, e$ )
22:  if  $s = 1$  and  $e = n_\sigma$  then
23:    for  $i = 2 \dots n_\sigma$  do
24:       $v_{i-1,i} = \max\{d_{i-1,i}/(t_i - t_{i-1} - \tau_{i-1}), v_F^*\}$ 

```

---

## 5. Computational Results

In this section, we evaluate the proposed MIHA on two sets of real-life data set. The presented algorithm was implemented in Matlab on a PC with an Intel Core i5-10400 processor, 16G RAM, and Microsoft Windows 10 operating system. The parameters used in our algorithm are listed in Table 2. We first test the MIHA on Beijing instance set, where the customer locations were scattered in both urban and suburban areas, and realistic geographical road information was leveraged to calculate the relevant costs [17]. Then experiments are conducted on larger-scale Jingdong instances. Twenty independent experiments were

conducted for each instance. Experimental results are listed in Tables 3–10, where the columns represent the best solution, the mean solution, the worst solution, the standard deviation (SD), and the elapsed time (ET, also known as computation time), respectively.

### 5.1. Parameter Analysis

#### 5.1.1. $p_{level3}$

In the level-3 membrane, an extra neighbourhood search was implemented with a specific probability  $p_{level3}$  to help find better solutions and improve the diversity of solutions. Here, we conducted the experiments on the Beijing example with 60 (customer) nodes, i.e., BJ60\_01, to analyse the influence of parameter  $p_{level3}$ , the results of which are recorded in Table 3. According to Table 3, either too low or too high probability deteriorated the performance. We suggest that lower probability was less effective in finding better solutions, while higher probability might lead the whole evolution to undesirable areas. Considering that the best overall result was captured at  $p_{level3} = 0.8$ , we used this value in the subsequent experiments.

**Table 2.** Algorithm parameters.

Notation	B	Typical Values
$I_{MCA}$	Iterations between MCAs	150
$I_{max}$	Maximum iteration number	500
$p_{level3}$	Probability of level-3 search	0.8
$Ar$	Archive size	100
$Ns$	Neighbourhood size	100
$L$	Tabu-list size	30
$P$	Population size	100
$p_{mutation}$	Rate of mutation	0.8
$p_{crossover}$	Rate of crossover	0.2
$(\alpha_1, \alpha_2, \mu, \lambda)$	$I_1$ parameters	(0.5, 0.5, 1, 1)

**Table 3.** Experimental result with different  $p_{level3}$ .

$p_{level3}$	Best Solution	Mean Solution	Worst Solution	SD	ET
0	10,875.6553	10,928.4416	10,957.5933	22.3405	98.4386
0.1	10,882.5664	10,935.8356	10,978.9560	25.6220	99.7357
0.2	10,897.0627	10,922.4866	10,946.9486	14.2856	106.7122
0.3	10,894.6855	10,935.1849	10,981.7598	22.6840	114.1316
0.4	10,893.8999	10,927.5347	10,960.1311	20.8581	132.3853
0.5	10,870.5658	10,927.1250	10,965.2899	28.0809	139.0837
0.6	10,893.7139	10,922.8795	10,946.2359	19.7116	153.5391
0.7	10,859.4377	10,918.7540	10,956.2807	23.5941	158.2609
0.8	10,849.7328	10,907.9905	10,959.0818	28.7783	172.7458
0.9	10,885.8673	10,922.2359	10,945.8091	16.2176	172.7154
1	10,864.7334	10,914.4491	10,939.8273	21.2864	179.3093

#### 5.1.2. $I_{MCA}$

As described previously, after a specific number of iterations each time, i.e.,  $I_{MCA}$ , the archive solutions of each level-2 membrane were sent to the skin membrane to help update the population. Here, the impact of parameter  $I_{MCA}$  is discussed. We still leveraged the same instance, i.e., BJ60\_01, to evaluate this parameter. As displayed in Table 4, the best result was captured at  $I_{MCA} = 150$ , which means that sending archive solutions of level-2 membranes to the skin membrane every 150 iterations achieved better performance.

Similarly, according to these results, either a smaller or larger  $I_{MCA}$  may deteriorate the solution; hence, we used  $I_{MCA} = 150$  in the subsequent experiments.

**Table 4.** Experimental results with different  $I_{MCA}$ .

$I_{MCA}$	Best Solution	Mean Solution	Worst Solution	SD	ET
15	10,887.9339	10,915.9258	10,933.9978	12.4846	180.9297
25	10,887.3386	10,907.1512	10,946.9533	17.9590	179.3292
50	10,864.7334	10,914.4491	10,939.8273	21.2864	179.3093
75	10,887.7475	10,914.0151	10,947.0650	18.9695	175.5044
100	10,899.9133	10,917.2956	10,930.3250	9.1312	174.3383
125	10,881.1171	10,913.0205	10,956.5405	19.0231	180.1102
150	10,847.0901	10,900.6532	10,947.3101	26.0596	150.6687
175	10,866.3854	10,908.5777	10,944.5708	23.6946	158.3528
200	10,878.1705	10,911.7143	10,945.2829	18.0546	184.6337

### 5.2. Effectiveness of Search in Level-3 Membranes

In this subsection, the effectiveness of the search in level-3 membranes is analyzed, where experiments were conducted on the Beijing 60-node instances with light-duty vehicles. The tabu search algorithm elicited desirable solutions faster by obtaining the attractor from the level-3 membranes. The MIHA without the level-3 membranes is denoted as  $MIHA_{level3}$  for convenience. The performance of MIHA and  $MIHA_{level3}$  on our example is shown in Table 5. It is easily observed that the level-3 membranes demonstrated considerable advantages in finding solutions with a lower total cost.

### 5.3. Effectiveness of Tabu Search

The tabu search algorithm plays a significant role in the level-2 membrane. In order to analyse the effectiveness of the tabu search algorithm, this part of the experiment used the greedy algorithm to replace the tabu search algorithm, i.e.,  $MIHA_{TS}$ , and compared the experimental results with MIHA. Although the membrane framework was retained in  $MIHA_{TS}$ , the demonstrated performance was less competitive than those achieved using MIHA, as shown in Table 6.

### 5.4. Effectiveness of GA in Skin Membrane

The crossover operator of the genetic algorithm can combine the excellent gene fragments of different individuals, and the mutation operator can help expand the search space. As an important part of the skin membrane, it is necessary to analyse the effectiveness of the genetic algorithm in the skin membrane. In MIHA, the solutions transmitted by the level-2 membranes formed the initial population of the skin membrane and finally output the excellent feasible solutions through the crossover and mutation operations in the genetic algorithm. In this subsection, MIHA without the genetic algorithm is denoted as  $MIHA_{GA}$ , in which the ability to integrate gene fragments from different membranes was absent, and the output was the best solutions from the level-2 membranes. Table 7 records the experimental results of both MIHA and  $MIHA_{GA}$ , respectively. The GA in the skin membrane had a favourable impact on the performance of our algorithm, as it achieved solutions with lower costs. Regarding the proposed MIHA, various solutions obtained by the tabu search of level-2 membranes with different attractors helped the GA escape from the local optimum. As a result, the cliffs were observed every  $I_{MCA}$  iterations in the convergence curve of the skin membrane, as depicted in Figure 6, which further justified the superiority of our design.

Table 5. Comparison of MIHA and MIHA<sub>level3</sub>.

	Instance	Best Solution	Mean Solution	Worst Solution	SD	ET
MIHA	BJ60_01	10,864.7334	10,914.4491	10,939.8273	21.2864	179.3093
	BJ60_02	10,217.4691	10,310.1949	10,395.6818	54.3404	167.1625
	BJ60_03	11,321.6848	11,423.8391	11,489.1644	53.3224	168.3861
	BJ60_04	11,800.7563	11,847.7284	11,915.0534	31.7880	179.6456
	BJ60_05	10,890.8377	10,909.8830	10,947.0117	14.5797	190.0507
	BJ60_06	11,875.3018	11,916.5380	11,942.8835	21.5401	157.5884
	BJ60_07	12,528.3080	12,634.5020	12,685.8953	54.0499	138.2126
	BJ60_08	11,783.3490	11,867.4716	11,932.7904	45.1478	162.5045
	BJ60_09	11,573.5410	11,705.3953	11,908.5312	107.6724	173.2149
	BJ60_10	12,939.9900	13,196.1938	13,269.0754	90.2917	161.0214
	Average	11,579.5971	11,672.6195	11,742.5914	49.4019	167.7096
MIHA <sub>level3</sub>	BJ60_01	10,876.9472	10,929.2492	10,959.7533	23.8597	99.9533
	BJ60_02	10,354.6481	10,439.4020	10,529.0454	47.3483	98.3095
	BJ60_03	11,417.6826	11,510.4497	11,651.4713	77.5482	99.3993
	BJ60_04	11,810.6944	11,850.3646	11,947.2880	36.0053	104.0135
	BJ60_05	10,900.3834	10,930.1086	10,996.6298	29.6276	115.6167
	BJ60_06	11,884.6734	11,934.8017	11,994.1760	37.2390	100.8201
	BJ60_07	12,570.4124	12,737.4635	12,916.3772	116.3777	88.5942
	BJ60_08	11,816.6496	11,865.4873	11,937.1039	42.1579	94.7336
	BJ60_09	11,652.5596	11,744.5783	11,860.8162	74.2931	92.3574
	BJ60_10	13,168.2194	13,240.3696	13,322.1267	43.8999	85.6219
	Average	11,645.2870	11,718.2275	11,811.4788	52.8356	97.9418

Table 6. Comparison of MIHA and MIHA<sub>TS</sub>.

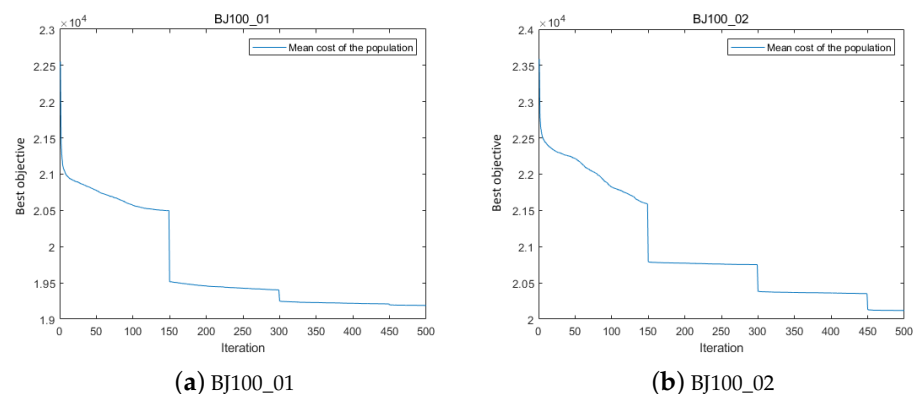
	Instance	Best Solution	Mean Solution	Worst Solution	SD	ET
MIHA	BJ60_01	10,864.7334	10,914.4491	10,939.8273	21.2864	179.3093
	BJ60_02	10,217.4691	10,310.1949	10,395.6818	54.3404	167.1625
	BJ60_03	11,321.6848	11,423.8391	11,489.1644	53.3224	168.3861
	BJ60_04	11,800.7563	11,847.7284	11,915.0534	31.7880	179.6456
	BJ60_05	10,890.8377	10,909.8830	10,947.0117	14.5797	190.0507
	BJ60_06	11,875.3018	11,916.5380	11,942.8835	21.5401	157.5884
	BJ60_07	12,528.3080	12,634.5020	12,685.8953	54.0499	138.2126
	BJ60_08	11,783.3490	11,867.4716	11,932.7904	45.1478	162.5045
	BJ60_09	11,573.5410	11,705.3953	11,908.5312	107.6724	173.2149
	BJ60_10	12,939.9900	13,196.1938	13,269.0754	90.2917	161.0214
	Average	11,579.5971	11,672.6195	11,742.5914	49.4019	167.7096
MIHA <sub>TS</sub>	BJ60_01	10,887.9165	10,928.7764	10,958.6152	22.1538	179.1811
	BJ60_02	10,350.4335	10,433.3471	10,569.4033	66.3863	165.9635
	BJ60_03	11,410.8506	11,546.6879	11,693.6700	83.6334	183.0199
	BJ60_04	11,808.0504	11,876.0743	12,002.3412	60.3121	190.7105
	BJ60_05	10,893.5351	10,908.2957	10,941.6042	15.4682	213.1253
	BJ60_06	11,930.4763	11,993.7405	12,040.6174	29.2162	162.8483
	BJ60_07	12,790.4131	12,945.8023	13,093.2836	95.8863	150.9155
	BJ60_08	11,840.7762	11,980.0637	12,070.6884	64.6119	170.2074
	BJ60_09	11,700.6390	12,040.8509	12,195.6716	140.5182	169.8237
	BJ60_10	13,352.3191	13,452.7316	13,528.2388	54.9095	152.6279
	Average	11,696.5410	11,810.6370	11,909.4134	63.3096	173.8423

**Table 7.** Comparison of MIHA and MIHA<sub>GA</sub>.

	Instance	Best Solution	Mean Solution	Worst Solution	SD	ET
MIHA	BJ60_01	10,864.7334	10,914.4491	10,939.8273	21.2864	179.3093
	BJ60_02	10,217.4691	10,310.1949	10,395.6818	54.3404	167.1625
	BJ60_03	11,321.6848	11,423.8391	11,489.1644	53.3224	168.3861
	BJ60_04	11,800.7563	11,847.7284	11,915.0534	31.7880	179.6456
	BJ60_05	10,890.8377	10,909.8830	10,947.0117	14.5797	190.0507
	BJ60_06	11,875.3018	11,916.5380	11,942.8835	21.5401	157.5884
	BJ60_07	12,528.3080	12,634.5020	12,685.8953	54.0499	138.2126
	BJ60_08	11,783.3490	11,867.4716	11,932.7904	45.1478	162.5045
	BJ60_09	11,573.5410	11,705.3953	11,908.5312	107.6724	173.2149
	BJ60_10	12,939.9900	13,196.1938	13,269.0754	90.2917	161.0214
	<i>Average</i>	11,579.5971	11,672.6195	11,742.5914	49.4019	167.7096
MIHA <sub>GA</sub>	BJ60_01	10,889.6733	10,920.5130	10,947.4318	20.3041	162.6233
	BJ60_02	10,267.1195	10,333.7142	10,415.6234	49.4848	149.6058
	BJ60_03	11,349.3097	11,473.1526	11,595.0291	77.7908	149.0490
	BJ60_04	11,804.8311	11,843.4759	11,937.9748	39.7545	150.1856
	BJ60_05	10,898.5533	10,917.0069	10,942.3023	14.3160	168.1142
	BJ60_06	11,882.7327	11,939.8357	11,973.6663	30.1972	170.9655
	BJ60_07	12,534.6436	12,658.8725	12,849.5941	85.0550	129.9516
	BJ60_08	11,806.8383	11,876.4740	11,934.8815	39.6358	138.7723
	BJ60_09	11,630.3241	11,687.7664	11,850.7900	63.9084	140.8432
	BJ60_10	13,120.3543	13,262.1483	13,355.0285	75.4520	128.9989
	<i>Average</i>	11,618.4380	11,691.2960	11,780.2322	49.5899	148.9109

### 5.5. Effectiveness of the Membrane Structure

In this subsection, we verify the effectiveness of the membrane structure. Generally, membrane computing provides a parallel distributed framework for solving the optimisation problem. We denoted our algorithm without the membrane structure as MIHA<sub>MS</sub>, in which all membranes were removed except for a single level-2 membrane, and the output was the best solution obtained by the algorithm in it. As shown in Table 8, without the membrane framework, the MIHA<sub>MS</sub> was far less effective in finding competitive solutions in comparison with the results obtained by using MIHA.

**Figure 6.** Cont.

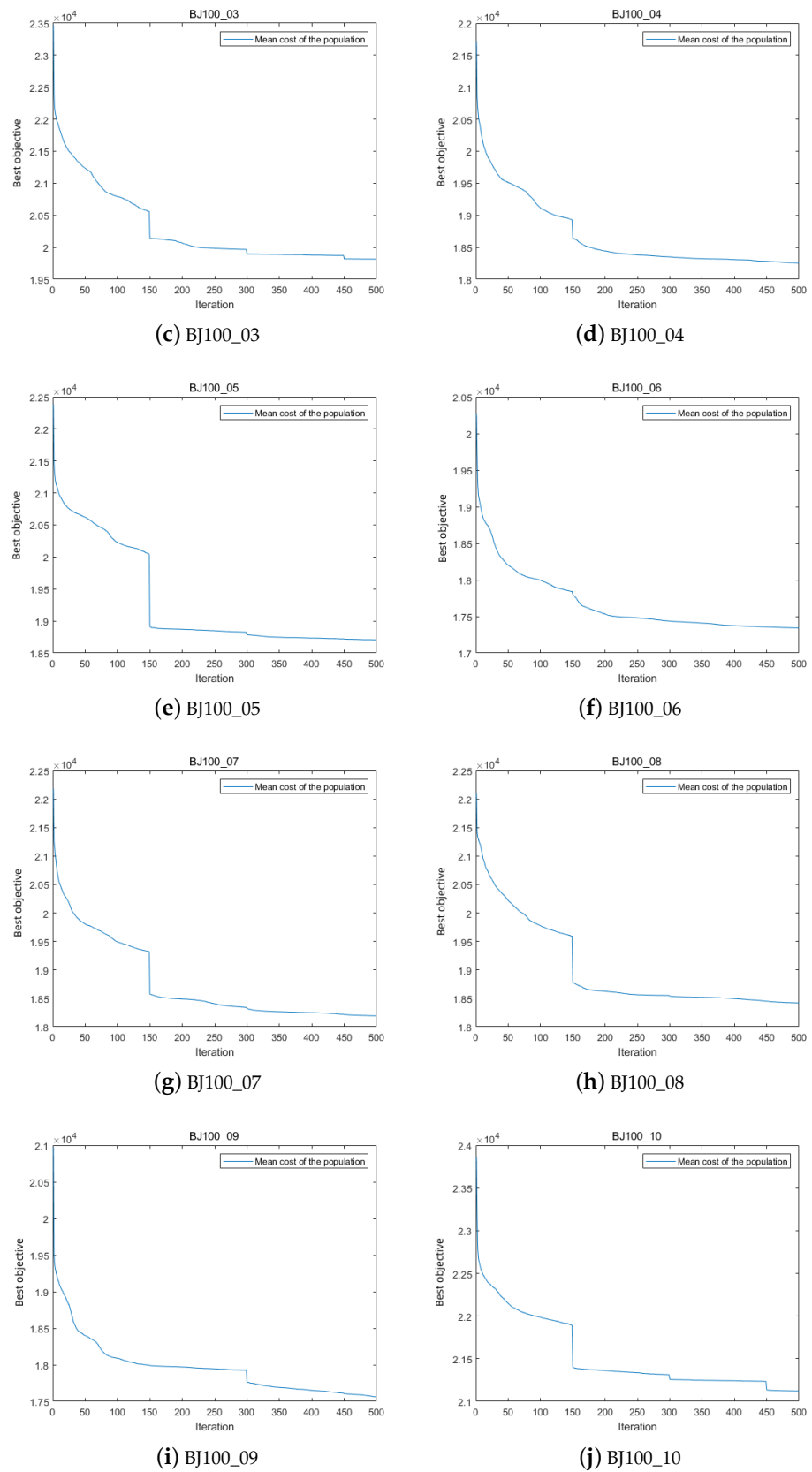


**Figure 6.** Convergence process of GA in skin membrane. (Cliffs are observed every  $I_{MCA}$  iterations in the convergence curves, which proves the effectiveness of the MCA.)

**Table 8.** Comparison of the MIHA and MIHA<sub>MS</sub>.

	Instance	Best Solution	Mean Solution	Worst Solution	SD	ET
MIHA	BJ60_01	10,864.7334	10,914.4491	10,939.8273	21.2864	179.3093
	BJ60_02	10,217.4691	10,310.1949	10,395.6818	54.3404	167.1625
	BJ60_03	11,321.6848	11,423.8391	11,489.1644	53.3224	168.3861
	BJ60_04	11,800.7563	11,847.7284	11,915.0534	31.7880	179.6456
	BJ60_05	10,890.8377	10,909.8830	10,947.0117	14.5797	190.0507
	BJ60_06	11,875.3018	11,916.5380	11,942.8835	21.5401	157.5884
	BJ60_07	12,528.3080	12,634.5020	12,685.8953	54.0499	138.2126
	BJ60_08	11,783.3490	11,867.4716	11,932.7904	45.1478	162.5045
	BJ60_09	11,573.5410	11,705.3953	11,908.5312	107.6724	173.2149
	BJ60_10	12,939.9900	13,196.1938	13,269.0754	90.2917	161.0214
	Average	11,579.5971	11,672.6195	11,742.5914	49.4019	167.7096
MIHA <sub>MS</sub>	BJ60_01	11,328.7061	11,450.7661	11,645.5626	102.4337	16.3996
	BJ60_02	10,706.7220	10,825.8266	10,952.4319	77.1375	16.0414
	BJ60_03	12,036.9001	12,135.7632	12,194.5568	54.3717	15.1175
	BJ60_04	12,367.3172	12,561.4857	12,854.7533	147.9147	17.2651
	BJ60_05	11,232.0918	11,294.0261	11,371.0893	52.7390	16.8575
	BJ60_06	12,288.4131	12,446.6655	12,589.8602	89.2907	16.7956
	BJ60_07	13,243.3081	13,393.8310	13,479.3281	84.1279	13.8604
	BJ60_08	12,172.4397	12,363.8495	12,507.0350	110.1176	13.1230
	BJ60_09	12,293.5838	12,422.8764	12,574.3870	75.6798	14.9571
	BJ60_10	13,356.4703	13,585.7384	13,783.8378	130.1142	13.2258
	Average	12,102.5952	12,248.0829	12,395.2842	92.3927	15.3643

### 5.6. Computational Result of Larger-Scale Problems

In this subsection, to further demonstrate the practical property of MIHA, the experiments were conducted on the larger-scale real-world problem instances, i.e., the Beijing 100-nodes set and the Jingdong 1000-nodes instance, respectively, where our method was set with  $p_{level3} = 0.8$  and  $I_{MCA} = 150$ . The results of the Beijing 100-nodes set are recorded in Table 9, and the results of the Jingdong 1000-nodes instance are recorded in Table 10. The computational result verified the favourable capability and superiority of the proposed MIHA in solving the real-world large-scale problem. In particular, in the comparison of different instance sizes, as shown in Table 11, a roughly linearly growing ET was observed, which justified the advantage of our algorithm in solving the large-scale problems.

**Table 9.** Computational result of the Beijing 100-node problem.

Instance	Best Solution	Mean Solution	Worst Solution	SD	ET
BJ100_01	19,067.0291	19,198.1247	19,286.2464	77.2545	177.5238
BJ100_02	20,054.6213	20,212.3116	20,335.2703	79.4795	177.5122
BJ100_03	19,611.4194	19,739.1057	19,807.4854	69.5798	187.4094
BJ100_04	18,185.2382	18,288.2393	18,365.8098	66.8545	183.9430
BJ100_05	18,450.2424	18,650.0880	18,721.6565	78.3719	177.8560
BJ100_06	17,185.9916	17,292.5207	17,429.9383	100.3186	191.1868
BJ100_07	18,018.7958	18,130.9018	18,231.9109	58.4036	203.7468
BJ100_08	18,077.4404	18,245.1333	18,386.8610	102.6939	190.7556
BJ100_09	17,317.3479	17,414.3330	17,513.4761	57.2721	181.7808
BJ100_10	20,888.4245	20,996.4199	21,191.1938	87.1091	165.4292
Average	18,685.6551	18,816.7178	18,926.9849	77.7338	183.7144

**Table 10.** Computational result of the Jingdong 1000-node problem.

Algorithm	Best Solution	Mean Solution	Worst Solution	SD	ET
MIHA	140,577.0284	141,085.6778	141,823.7589	365.4070	2331.9363

**Table 11.** The mean elapsed time of different instance sizes.

Instance	BJ60	BJ100	JD1000
ET	150.6687	183.7144	2331.9363

5.7. Comparison with Other Algorithms

Three heuristic algorithms, i.e., the hybrid tabu search [17], the tabu search, and the GA [33] were implemented as baselines to compare with our MIHA, the results of which are recorded in Figures 7 and 8. From Figure 7, we see that MIHA outperformed the hybrid tabu search, the tabu search, and the GA in terms of solution quality and convergence speed for all ten instances of BJ100, respectively. Moreover, Figure 8 shows the results of the four algorithms for the JD1000 instance, where our MIHA not only achieved the lowest cost but also presented the highest convergence speed. This further demonstrates the significant advantage of MIHA in solving a large-scale problem.

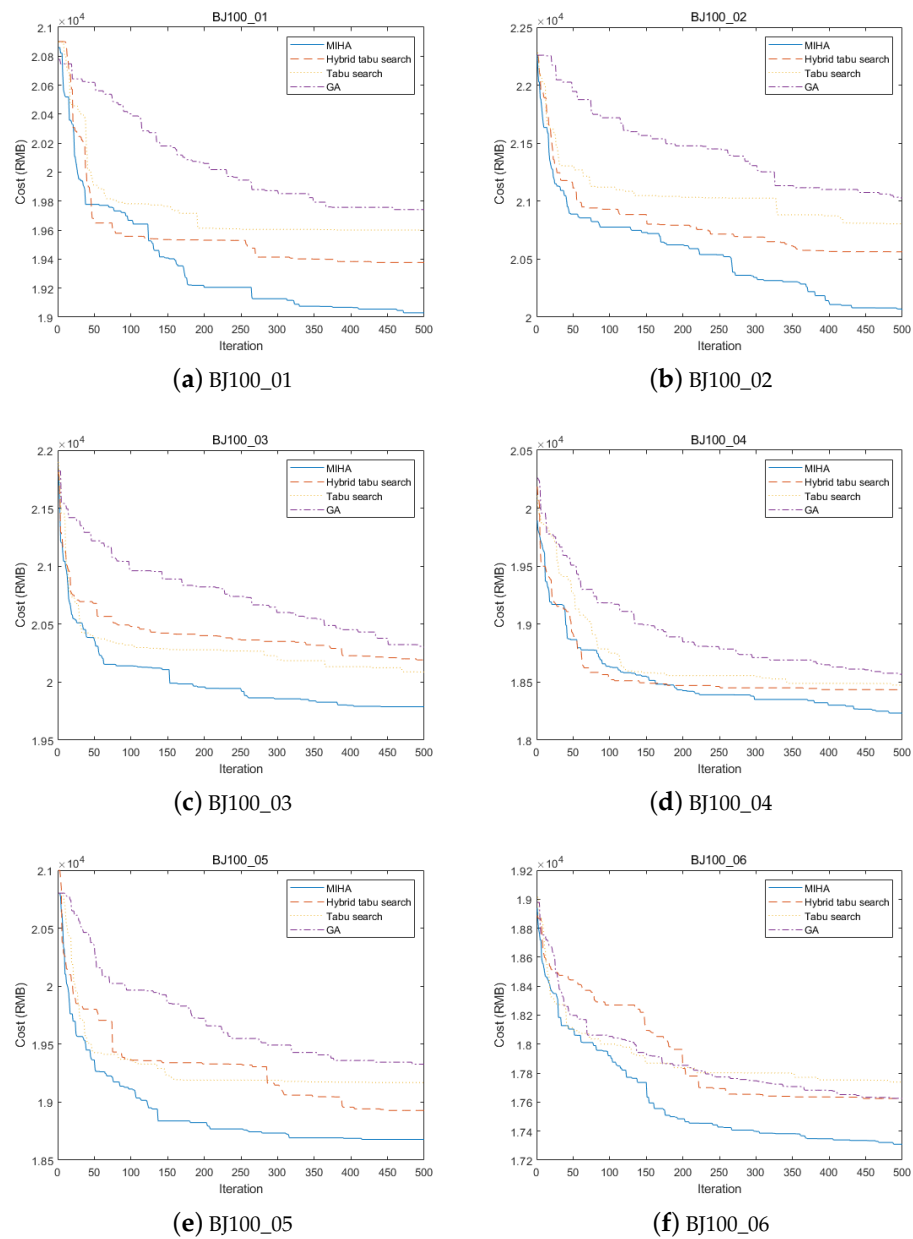


**Figure 7.** Cont.

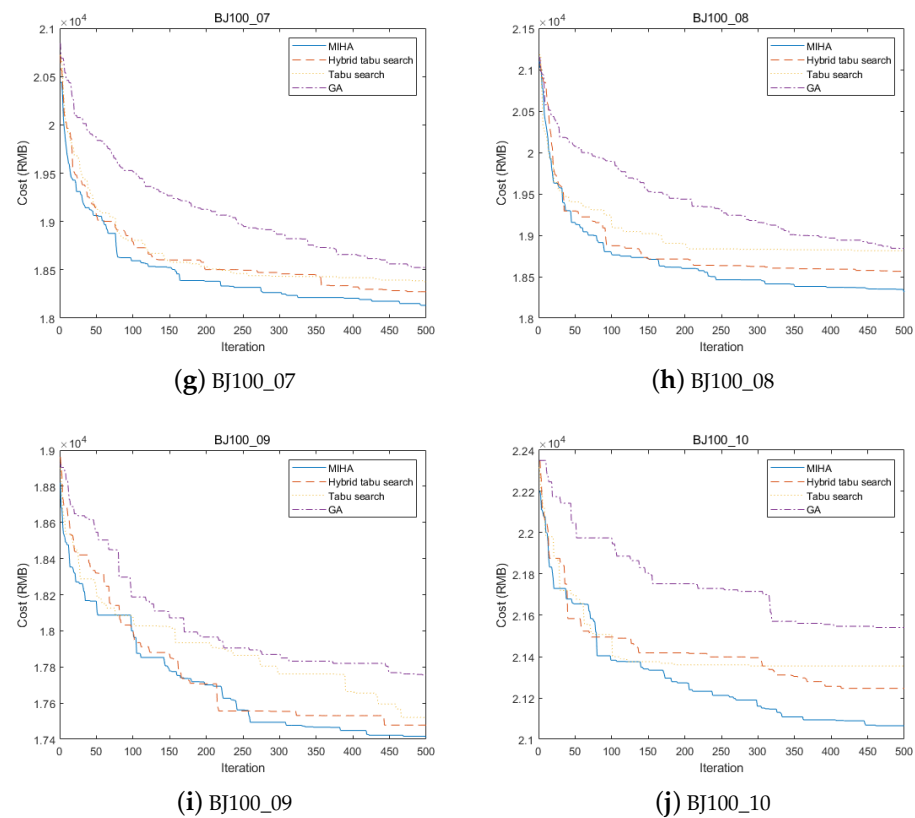


**Figure 7.** The convergence curves of the MIHA, hybrid Tabu search, Tabu search, and GA for 10 instances of BJ100. (The MIHA outperforms other algorithms in terms of solution quality and convergence speed in all instances of BJ100.)

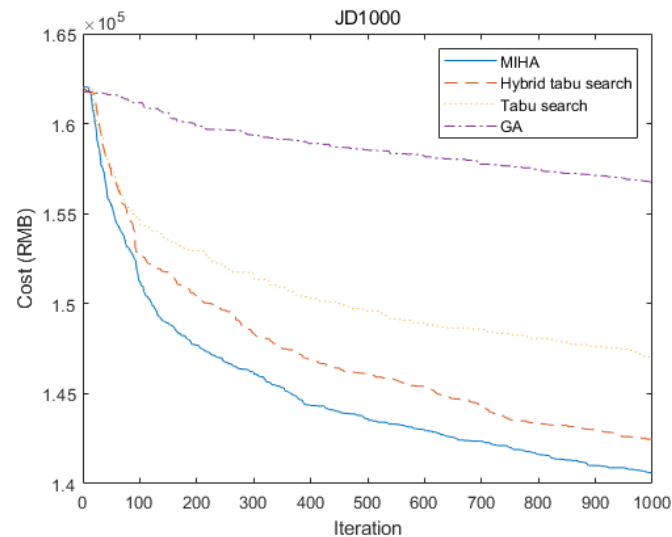


**Figure 8.** The convergence curves of MIHA, hybrid tabu search, tabu search, and GA for the JD1000 problem instance.

## 6. Conclusions

In this paper, we designed a membrane-inspired framework to improve the performance of the heuristics when dealing with a realistic and large-scale green open vehicle routing problem with time windows. The proposed method, i.e., a membrane-inspired hybrid algorithm, benefits from the parallel distributed structure and a unique communication strategy in the P system. The computational results based on the Beijing dataset and

Jingdong instance justified its strong competitiveness against other baselines, where our algorithm achieved the lowest overall cost, which comprises fuel cost, emission cost, and driver cost, on all tested instances.

The green open vehicle routing problem with time windows, as a notable variant of the vehicle routing problem, has considerable value in the vigorous development of the sharing economy, green logistics, and sustainable society. In the future, more realistic models involving the green open routes will be investigated, such as the green close–open vehicle routing problem and variants that consider a heterogeneous fleet. Our algorithm might still be able to solve them with appropriate modifications, given the desirable generalisation capability of the membrane-inspired algorithms for solving hard optimisation problems. We also plan to integrate our work with the deep (reinforcement)-learning-based methods developed by Li et al. [49], Wu et al. [50], and Xin et al. [51] for solving routing problems, so that it allows the membrane-inspired algorithms to be more intelligent. In addition, the engine of the vehicle poses many advantages to improve the performance and parameter characteristics [52], and carbon emissions can be reduced if an appropriate injection strategy is adopted [53]. Therefore, the improvement of the engine should be considered in future work. Future research directions can also focus on developing more optimisation methods such as the lion optimisation algorithm [54], red deer algorithm [55], etc.

**Author Contributions:** Conceptualization, Y.N. and Z.Y.; methodology, Y.N., Z.Y and J.X.; writing—original draft preparation, Z.Y.; writing—review and editing, R.W.; supervision, S.Z.; funding acquisition, Y.N. and J.X. All authors have read and agreed to the published version of the manuscript.

**Funding:** This work was supported by the National Natural Science Foundation of China [grant numbers 62172373, 61872325, 62072258, 61772290] and the Fundamental Research Funds for the Central Universities, China [grant number 2652019028].

**Institutional Review Board Statement:** Not applicable.

**Informed Consent Statement:** Not applicable.

**Data Availability Statement:** The data presented in this study are available on request from the corresponding author.

**Conflicts of Interest:** The authors declare no conflict of interest.

## Notations

$G$	Complete directed graph
$N$	Node set
$N_0$	Customer set
$A$	Arc set
$Q$	Vehicle capacity
$w$	The weight of a vehicle
$q_i$	The demand of customer $i$
$s_i$	The time cost of the route ending with $i$
$y_i$	The actual starting time for serving node $i$
$d_{ij}$	The length of arc $(i, j)$
$f_{ij}$	The amount of freight flow on arc $(i, j)$
$x_{ij}$	Binary flag variable 1
$z_{ij}^r$	Binary flag variable 2
$v_{ij}^r$	The travel speed of vehicle $r$ on arc $(i, j)$
$[a_i, b_i]$	The time window of customer $i$

## References

1. Dantzig, G.B.; Ramser, R.H. The truck dispatching problem. *Manag. Sci.* **1959**, *6*, 80–91. [[CrossRef](#)]
2. Long, J.; Sun, Z.; Pardalos, P.M.; Hong, Y.; Zhang, S.; Li, C. A hybrid multi-objective genetic local search algorithm for the prize-collecting vehicle routing problem. *Inf. Sci.* **2019**, *478*, 40–61. [[CrossRef](#)]

3. Zhang, D.; Cai, S.; Ye, F.; Si, Y.; Nguyen, T.T. A hybrid algorithm for a vehicle routing problem with realistic constraints. *Inf. Sci.* **2017**, *394*, 167–182. [[CrossRef](#)]
4. Toth, P.; Vigo, D. *The Vehicle Routing Problem*; Society for Industrial and Applied Mathematics: Philadelphia, PA, USA, 2002; p. 9.
5. Repoussis, P.P.; Tarantilis, C.D.; Ioannou, G. The open vehicle routing problem with time windows. *J. Oper. Res.* **2007**, *58*, 355–367. [[CrossRef](#)]
6. Moghdani, R.; Salimifard, K.; Demir, E.; Benyettou, A. The green vehicle routing problem: A systematic literature review. *J. Clean. Prod.* **2021**, *279*, 123691. [[CrossRef](#)]
7. Bodin, L.; Golden, B.; Assad, A.; Ball, M. Routing and scheduling of vehicles and crews: The state of the art. *Comput. Oper. Res.* **1983**, *10*, 63–211.
8. Brandao, J. A tabu search heuristic algorithm for open vehicle routing problem. *Eur. J. Oper. Res.* **2004**, *157*, 552–564. [[CrossRef](#)]
9. Fleszar, K.; Osman, I.H.; Hindi, K.S. A variable neighbourhood search algorithm for the open vehicle routing problem. *Eur. J. Oper. Res.* **2009**, *195*, 803–809. [[CrossRef](#)]
10. Tarantilis, C.D.; Ioannou, G.; Kiranoudis, C.T.; Prastacos, G.P. Solving the open vehicle routing problem via a single parameter meta-heuristic algorithm. *J. Oper. Res.* **2005**, *56*, 588–596. [[CrossRef](#)]
11. MirHassani, S.; Abolghasemi, N. A particle swarm optimization algorithm for open vehicle routing problem. *Expert Syst. Appl.* **2011**, *38*, 11547–11551. [[CrossRef](#)]
12. Li, X.; Tian, P.; Leung, S. An ant colony optimization metaheuristic hybridized with tabu search for the open vehicle routing problem. *J. Oper. Res. Soc.* **2009**, *60*, 1012–1025. [[CrossRef](#)]
13. Repoussis, P.P.; Tarantilis, C.D.; Braysy, O.; Ioannou, G. A hybrid evolution strategy for the open vehicle routing problem. *Comput. Oper. Res.* **2010**, *37*, 443–455. [[CrossRef](#)]
14. Ashtineh, H.; Pishvae, M. Alternative Fuel Vehicle-Routing Problem: A life cycle analysis of transportation fuels. *J. Clean. Prod.* **2019**, *219*, 166–182. [[CrossRef](#)]
15. Yu, Y.; Wang, S.; Wang, J.; Huang, M. A branch-and-price algorithm for the heterogeneous fleet green vehicle routing problem with time windows. *Transp. Res. Part B Methodol.* **2019**, *122*, 511–527. [[CrossRef](#)]
16. Wang, L.; Lu, J. A memetic algorithm with competition for the capacitated green vehicle routing problem. *IEEE/CAA J. Autom. Sin.* **2019**, *6*, 516–526. [[CrossRef](#)]
17. Niu, Y.; Yang, Z.; Chen, P.; Xiao, J. Optimizing the green open vehicle routing problem with time windows by minimizing comprehensive routing cost. *J. Clean Prod.* **2018**, *171*, 962–971. [[CrossRef](#)]
18. Pan, L.; Păun, Gh; Pérez-Jiménez, M.J. Spiking neural P systems with neuron division and budding. *Sci. China Inf. Sci.* **2011**, *54*, 1596–1607. [[CrossRef](#)]
19. Păun, G. Computing with membranes. *J. Comput. Syst. Sci.* **2000**, *61*, 108–143. [[CrossRef](#)]
20. Sosík, P. P systems attacking hard problems beyond NP: A survey. *J. Membr. Comput.* **2019**, *1*, 198–208 [[CrossRef](#)]
21. Ciobanu, G.; Pérez-Jiménez, M.J.; Păun, G. (Eds.) *Applications of Membrane Computing*; Springer: Berlin/Heidelberg, Germany, 2006; Volume 287, pp. 73–100.
22. Derigs, U.; Reuter, K. A simple and efficient tabu search heuristic for solving the open vehicle routing problem. *J. Oper. Res. Soc.* **2009**, *60*, 1658–1669. [[CrossRef](#)]
23. Fu, Z.; Eglese, R.; Li, L. Corrigendum to the paper: A new tabu search heuristic for the open vehicle routing problem. *J. Oper. Res. Soc.* **2006**, *57*, 1017–1018. [[CrossRef](#)]
24. Russell, R.; Chiang, W.; Zepeda, D. Integrating multi-product production and distribution in newspaper logistics. *Comput. Oper. Res.* **2008**, *35*, 1576–1588. [[CrossRef](#)]
25. Pisinger, D.; Ropke, S. A general heuristic for vehicle routing problems. *Comput. Oper. Res.* **2007**, *34*, 2403–2435. [[CrossRef](#)]
26. Salari, M.; Toth, P.; Tramontani, A. An ILP improvement procedure for the open vehicle routing problem. *Comput. Oper. Res.* **2010**, *37*, 2106–2120. [[CrossRef](#)]
27. Zachariadis, E.; Kiranoudis, T. An open vehicle routing problem metaheuristic for examining wide solution neighbourhoods. *Comput. Oper. Res.* **2010**, *37*, 712–723. [[CrossRef](#)]
28. Tarantilis, C.D.; Ioannou, G.; Kiranoudis, C.T.; Prastacos, G.P. A threshold accepting approach to the open vehicle routing problem. *RAIRO Oper. Res.* **2004**, *38*, 345–360. [[CrossRef](#)]
29. Wang, W.; Wu, B.; Zhao, Y.; Feng, D. Particle swarm optimization for open vehicle routing problem. In *International Conference on Intelligent Computing: Part II*; Huang, D.S., Li, K., Irwin, G.W., Eds.; Springer: Berlin/Heidelberg, Germany, 2006; pp. 999–1007.
30. Zhen, T.; Zhu, Y.; Zhang, Q. A particle swarm optimization algorithm for the open vehicle routing problem. In *Proceedings of the 2009 International Conference on Environmental Science and Information Application Technology*, Wuhan, China, 4–5 July 2009; pp. 560–563.
31. Li, X.; Tian, P. An ant colony system for the open vehicle routing problem. In *Lecture Notes in Computer Science (ANTS 2006)*; Dorigo, M., Ed.; Springer: Berlin/Heidelberg, Germany, 2006; Volume 4150, pp. 356–363.
32. Pan, L.; Fu, Z. A clonal selection algorithm for open vehicle routing problem. In *Proceedings of the 2009 Third International Conference on Genetic and Evolutionary Computing*, Guilin, China, 14–17 October 2009; pp. 786–790.
33. Yu, S.; Ding, C.; Zhu, K. A hybrid GA-TS algorithm for open routing optimization of coal mines material. *Expert Syst. Appl.* **2011**, *38*, 10568–10573. [[CrossRef](#)]

34. Barbuti, R.; Bove, P.; Milazzo, P.; Pardini, G. Minimal probabilistic P systems for modelling ecological systems. *Theor. Comput. Sci.* **2015**, *608*, 36–56. [[CrossRef](#)]
35. Lucie, C.; Erzsébet, C.; Ludxexk, C.; Petr, S. P colonies. *J. Membr. Comput.* **2019**, *1*, 178–197.
36. Niu, Y.; Zhang, Y.; Zhang, J. Running cells with decision-making mechanism: intelligence decision P System for evacuation simulation. *Int. J. Comput. Commun.* **2018**, *13*, 865–880. [[CrossRef](#)]
37. Sakellariou, I.; Stamatopoulou, I.; Kefalas, P. Using membranes to model a multi-agent system towards underground metro station crowd behaviour simulation. In Proceedings of the ECAI 2012 Workshop, Montpellier, France, 28 August 2012; pp. 5–10.
38. Nishida, T.Y. Membrane algorithms: Approximate algorithms for NP-complete optimization problems. In *Applications of Membrane Computing*; Springer: Berlin/Heidelberg, Germany, 2006; pp. 303–314.
39. Zhang, G.; Liu, C.; Rong, H. Analyzing radar emitter signals with membrane algorithms. *Math. Comput. Model.* **2010**, *52*, 1997–2010. [[CrossRef](#)]
40. Zhang, G.; Rong, H.; Neri, F.; Pérez-Jiménez, M.J. An optimization spiking neural P system for approximately solving combinatorial optimization problems. *Int. J. Neural. Syst.* **2014**, *24*, 1440006. [[CrossRef](#)] [[PubMed](#)]
41. Zhang, G.; Rong, H.; Cheng, J.; Qin, Y. A population-membrane-system-inspired evolutionary algorithm for distribution network reconfiguration. *J. Electron.* **2014**, *23*, 437–441.
42. Barth, M.; Boriboonsomsin, K. Energy and emissions impacts of a freeway-based dynamic eco-driving system. *Transp. Res. Part D* **2009**, *14*, 400–410. [[CrossRef](#)]
43. Barth, M.; Younglove, T.; Scora, G. *Development of a Heavy-Duty Diesel Modal Emissions and Fuel Consumption Model*; Technical Report; UCB-ITS-PRR-2005-1, California PATH Program; Institute of Transportation Studies, University of California at Berkeley: Berkeley, CA, USA, 2005.
44. Scora, M.; Barth, G. Comprehensive Modal Emission Model (CMEM), Version 3.01, User Guide. Technical Report. 2006. Available online: [http://www.cert.ucr.edu/cmem/docs/CMEM\\_User\\_Guide\\_v3.01d.pdf](http://www.cert.ucr.edu/cmem/docs/CMEM_User_Guide_v3.01d.pdf) (accessed on 17 February 2014).
45. Koç, Ç.; Bektaş, T.; Jabali, O.; Laporte, G. The fleet size and mix pollution-routing problem. *Transp. Res. Part B Methodol.* **2014**, *70*, 239–254. [[CrossRef](#)]
46. Tan, K.C.; Cheong, C.K.; Goh, C.K. Solving multi-objective vehicle routing problem with stochastic demand via evolutionary computation. *Eur. J. Oper. Res.* **2007**, *177*, 813–839. [[CrossRef](#)]
47. Solomon, M.M. Algorithms for the vehicle routing and scheduling problems with time window constraints. *Oper. Res.* **1987**, *35*, 254–265. [[CrossRef](#)]
48. Kramer, M.; Maculan, N.; Subramanian, A.; Vidal, T. A speed and departure time optimization algorithm for the pollution-routing problem. *Eur. J. Oper. Res.* **2015**, *247*, 782–787. [[CrossRef](#)]
49. Li, J.; Xin, L.; Cao, Z.; Lim, A.; Song, W.; Zhang, J. Heterogeneous Attention for Solving Pickup and Delivery Problem via Deep Reinforcement Learning. *IEEE Trans. Intell. Transp. Syst.* **2021**, *23*, 2306–2315. [[CrossRef](#)]
50. Wu, Y.; Song, W.; Cao, Z.; Zhang, J.; Lim, A. Learning Improvement Heuristics for Solving Routing Problems. *IEEE Trans. Neural Netw. Learn. Syst.* **2021**, 1–13. [[CrossRef](#)]
51. Xin, L.; Song, W.; Cao, Z.; Zhang, J. Step-wise deep learning models for solving routing problems. *IEEE Trans. Ind. Inform.* **2020**, *17*, 4861–4871. [[CrossRef](#)]
52. Shi, C.; Zhang, Z.; Ji, C.; Li, X.; Di, L.; Wu, Z. Potential improvement in combustion and pollutant emissions of a hydrogen-enriched rotary engine by using novel recess configuration. *Chemosphere* **2022**, *299*, 134491. [[CrossRef](#)]
53. Shi, C.; Ji, C.; Ge, Y.; Wang, S.; Wang, H.; Yang, J. Parametric analysis of hydrogen two-stage direct-injection on combustion characteristics, knock propensity, and emissions formation in a rotary engine. *Fuel* **2021**, *287*, 119418. [[CrossRef](#)]
54. Menaga, D.; Revathi, S. Least lion optimisation algorithm (LLOA) based secret key generation for privacy preserving association rule hiding. *IET Inf. Secur.* **2018**, *12*, 332–340. [[CrossRef](#)]
55. Fathollahi-Fard, A.M.; Hajiaghayi-Keshteli, M.; Tavakkoli-Moghaddam, R. Red deer algorithm (RDA): A new nature-inspired meta-heuristic. *Soft Comput.* **2020**, *24*, 14637–14665. [[CrossRef](#)]